

***Ab initio* study of Schottky barriers at metal-nanotube contacts**

Bin Shan

Department of Applied Physics, Stanford University, Stanford, California 94305, USA

Kyeongjae Cho*

Department of Mechanical Engineering, Stanford University, Stanford, California 94305, USA

(Received 12 August 2004; published 9 December 2004)

The type of barrier at a metal/CNT junction is one of the key issues in nanotube electronics. Despite the extensive experimental work done to clarify this issue, there is no consensus in the nano-electronics community. We present here the first *ab initio* calculation on the Schottky barrier and tunneling barrier height of an idealized metal (Au, Pd, Pt) semiconducting (8,0) nanotube junction. All three metal species form Schottky barriers when contacting small diameter nanotubes. Two most important atomic geometrical factors influencing the Schottky barrier height are identified as the metal species and its surface orientation. Pd is found to have the lowest Schottky barrier. Our simulation results give useful insight into the on going experiments.

DOI: 10.1103/PhysRevB.70.233405

PACS number(s): 73.40.Ns, 72.80.Rj, 31.15.Ar

Carbon nanotube field-effect transistors (CNTFETs) are one of the most promising candidates to continue the miniaturization of microelectronics to a new level, due to their small size, reliable structural strength and mature synthesis methods. Some of their capabilities and performance have already been demonstrated.¹ The continued improvement of their device characteristics requires a good understanding of the metal/CNT junction, which unfortunately is still lacking. Depending on the junction property, the CNT-FET can either operate in ways similar to conventional MOSFETs (Ohmic junction),³ or operate as unconventional Schottky barrier transistors (Schottky junction) as the IBM group has recently proposed.² Several papers have shown that the scaling law for MOSFET and Schottky-barrier (SB) CNTFETs show significant differences.^{3,4}

There have been many experiments done trying to clarify this issue, most of which are transport measurements. Au, Pd and Pt are popular high work function metals for such *p*-type conductance measurements.⁵⁻⁹ The measurements up till now are, however, highly controversial. The IBM group found that a SB exists independent of the metal species being used,² while Dai group recently achieved conductance approaching ballistic transport limit using Pd as contact material,^{5,6} indicating a small or negative Schottky barrier at the Pd/CNT contact. The case of Au contact is also controversial. In previous experiments, the ON conductance fell well below the conductance quanta $4e^2/h$.^{7,8} Some recent experiments indicate that Au makes good contact,⁹ with a relatively high ON conductance around 1/3 of the conductance quanta. It is not yet clear however, whether the low conductance in the ON state is due to intrinsic SB at the junction or some external imperfections in the experiment.

Many theoretical efforts also have been devoted to the contact problem, but usually in a semiempirical manner that to some extent ignores the microscopic description of the contact. The metal-induced gap states (MIGS)¹⁰ model, for example, predicts a Schottky barrier (SB) that is only dependent on the band structure of the semiconductor. However, in order to fully account for the detailed charge transfer at the highly inhomogeneous metal/CNT contact region, it is nec-

essary to model the contact on the atomic scale. To this end, we carried out first principle total energy calculations using the pseudopotential plane wave method¹¹ within local density approximation (LDA). The calculations are done in supercell geometry containing one unit of semiconducting (8,0) CNT and a metal slab of five atomic layers. Metals of different species (Au, Pd, Pt) and orientations (111,100) are studied. Schottky barrier height (SBH) at the metal/CNT interface as well as its dependence on atomic geometries are determined using the method of potential profile lineup.¹³ Due to the periodicity constraint, the metal slabs are either compressed (111 surface) or elongated (100 surface) to match the lattice constant of (8,0) SWNT unit cell. The induced strain/stress perpendicular to the CNT axis are calculated using bulk Poisson's ratio. The strain/stress is then minimized by varying the lattice constant of the metal slab as was done in Ref 12 and 13. Our simulation results show that SBH depends on both the metal species and the surface orientation of the metal slab. These effects are not captured within the MIGS¹⁰ model and signify the importance of modeling the ultrascale metal/CNT junction on the atomic scale. In Au/CNT contact, the modulation of the SBH due to atomic geometry is most pronounced and can be as high as 0.2 eV. This possibly gives rise to the large variations in conductance observed at Au/CNT contact. Pd has the lowest SBH and strongest bonding to the CNT, revealing itself to be a good candidate for making transparent contact to CNT.

Only *side-contact* geometry is considered in this study. This is one of the most probable geometries for metal/CNT contact, since the contact is formed by either placing the tube on top of predefined metal electrodes or by depositing metal electrodes onto the CNT lying on the substrate.¹⁴ The other possibility is *end-contact* geometry.¹⁵ It is shown that in *end-contact* geometry, Fermi-level pinning effect cannot control the device property,¹⁶ and we have not extended our modeling study to the end-contact geometry. Geometry optimizations are done in two steps. First, we sample over various geometries of interest while freezing other degrees of freedom. From the partially optimized geometries, the most energetically favorable geometry is chosen, and a subsequent

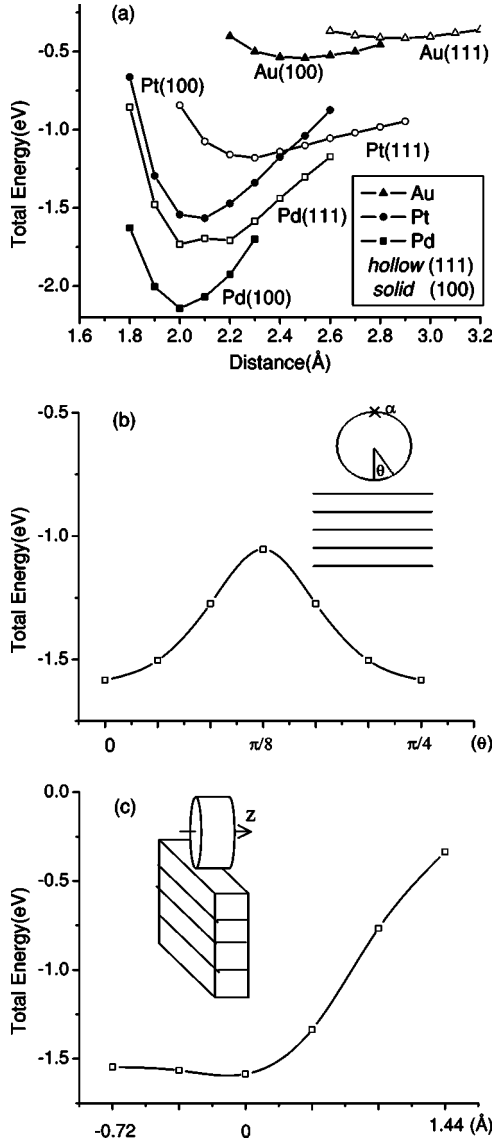


FIG. 1. Total energy of metal/CNT as a function of (a) interfacial distance, (b) rotational angle, (c) translation along tube axis. The reference energy is taken as metal/CNT separated by infinite distance. Pt(100) curve in (a) is shifted up 0.2 eV for clarity.

full *ab initio* optimization was done to relax the entire structure, with the bottom two metal layers fixed. This two-step optimization ensures we have reasonable ground state geometry to work with rather than being trapped at some high energy local minima. Major degrees of freedom sampled include metal/CNT distance, CNT rotation, and relative metal/CNT translation. Most possible contact geometries such as DT (direct on top), BM (bridge middle), and HC (hexagonal center)¹⁷ can all be characterized by these degrees of freedom. Figure 1(a) shows the total energy for DT geometry as a function of interfacial distance. We see from the total energy curve that the interaction strength between metal/CNT is Pd > Pt > Au. The confinement potential is shallow for Au/CNT while sharp for Pd/CNT contact. Thus smaller energy is needed for the equilibrium Au/CNT distance to vary compared with the other two metals. Two local minima on the total energy curve for Pd(111) surface is due to the compe-

TABLE I. Binding energy and Schottky barrier at equilibrium distances.

Metal (Orientation)	Equilibrium binding distance (Å)	Binding energy (eV)	Schottky barrier (eV)
Au(111)	2.91	0.61	0.23
Au(100)	2.40	0.74	0.42
Pd(111)	2.12	2.00	0.26
Pd(100)	2.04	2.70	0.15
Pt(111)	2.12	1.69	0.35
Pt(100)	2.10	2.30	0.29

tion between nearest Pd/C bond (one bond per unit cell) and second nearest Pd/C bonds (two bonds per unit cell). These two nearly degenerate local minima collapse into one minimum when we allow full relaxation of the structure. Upon relaxation, Pd(111) surface finally equilibrates with CNT at a distance of 2.12 Å. Figures 1(b) and 1(c) show the energy dependence on rotation angle and translation along the CNT axis for Pd(111)/CNT at its equilibrium distance. Table I summarizes the equilibrium distance, binding energy and Schottky barrier height of metal/CNT systems at fully optimized geometries. The local atomic relaxations generally lower the total energy by ~0.3 eV, but has little effect on SBH. Pd has the highest binding energy among them, which is in agreement with experiment that Pd has a much higher sticking coefficient than other metals and forms a uniform coating on the CNT.¹⁸

Schottky barrier between metal and semiconductor (Al/GaAs) has been studied before using methods of potential profile lineup.¹³ Here, we use similar approach with slight modification. The *p*-type Schottky barrier ΔE_p can be expressed as the difference between the Fermi level of the system and the valence band edge of the semiconductor,

$$\Delta E_p = E_F - E_V = \{E_F - \langle V \rangle_{\text{CNT}}\} - \{E_V - \langle V \rangle_{\text{CNT}}\}. \quad (1)$$

In order to deduce the valence band edge of the nanotube, we introduce $\langle V \rangle$ which denotes the average potential at corresponding atomic core. The first term in parentheses is extracted from a self-consistent calculation, which fully incorporates the effects of atomic rearrangements and charge redistribution. $\langle V \rangle_{\text{CNT}}$ is evaluated at carbon site α furthest away from the interface [marked on the inset of Fig. 1(b)]. This average potential however, deviates from that in an isolated nanotube due to charges spilled to/from the metal contact. Integrating the charge density within the Wigner-Seitz radius at the carbon site α shows that the net charge transfer is zero. So this deviation is expected to be small. The correction due to possible charge distribution distortion is evaluated using single metal atom interacting with a long CNT and comparing the average potential difference between site α carbon and carbon deep inside the nanotube. For Pd/CNT, where there is significant charge transfer at the interface, the deviation is less than 0.01 eV. This correction term is included in the final SBH result. The second term in Eq. (1) is deduced from an individual CNT calculation without metal

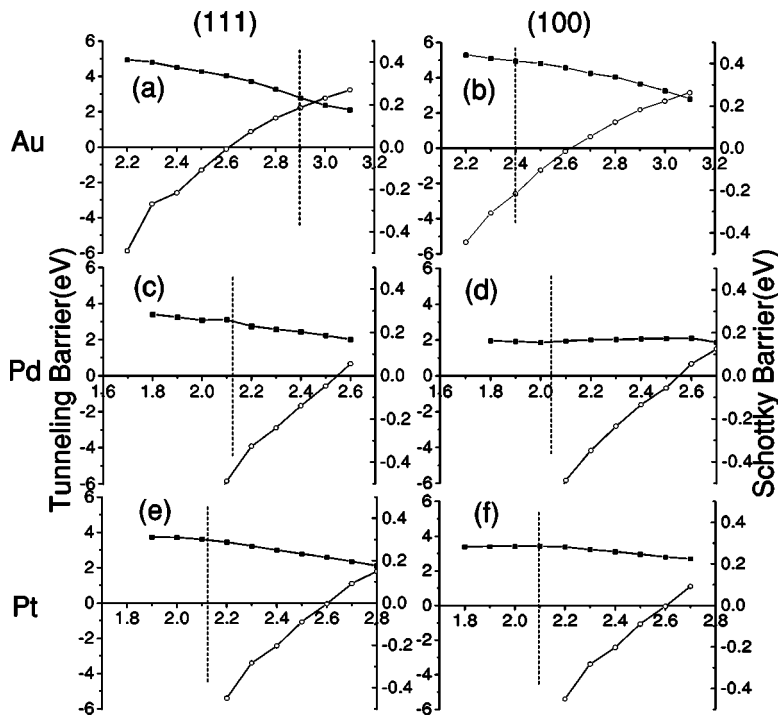


FIG. 2. Schottky barrier height and tunneling barrier height for different metal/(8,0)CNT combinations as a function of interfacial distance. Solid squares indicate Schottky barrier height (right axis) and empty dots indicates tunneling barrier height (left axis). Dashed line indicates equilibrium distance (a) Au(111)/CNT, (b) Au(100)/CNT, (c) Pd(111)/CNT, (d) Pd(100)/CNT, (e) Pt(111)/CNT, (f) Pt(100)/CNT

electrode. As pointed out in Ref. 13, this term may contain errors due to LDA approximation being used, but changes in Schottky barrier height due to atomic relaxations are essentially ground state property and can be modeled quite accurately within LDA.

We show in Fig. 2 the dependence of SBH as a function of interfacial distance for different metal surfaces interacting with (8,0) CNT. When contacting to small (8,0) nanotubes, all three metals exhibit SB's and the direction of charge transfer is from CNT to metal. SBH is generally a monotonously decreasing function of interfacial distance, with saturation sets on going to smaller distances. The exact value of SBH depends highly on both the metal species and its surface orientation. We clearly see in the Au/CNT case how atomic details like different crystalline orientations can be important in determining SBH. As indicated in Figs. 2(a) and 2(b), (100) oriented gold surface is more reactive than (111) surface and equilibrates with CNT at a shorter distance. This smaller binding distance enhances the dipole moment that pulls down the energy levels on the CNT side with respect to the metal side. Thus the Fermi level of Au (100) at equilibrium distance is pinned at a higher position in the band gap than that of the Au (111) surface. The modulation of SBH by changing equilibrium interfacial distance is most pronounced in the Au/CNT case, as high as 0.2 eV. Also due to the shallow confinement potential at Au/CNT contact, the interfacial distance is subject to relatively large fluctuations. The SBH can be either highest among three metals at short binding distance [Au(100)/CNT] or comparatively low when it equilibrates at a larger distance [Au(111)/CNT]. However, in this particular case, as the SBH gets smaller by increasing the interfacial distance, a finite tunneling barrier (SCF electronic potential barrier seen by the electrons at Fermi level) may develop at the interface. The tunneling barrier is localized at the interface bonds and narrow in width ~ 0.65 Å, the

tunneling probability at equilibrium distance estimated by WKB approximation is ~ 0.39 . This potential barrier gives rise to an intrinsic contact resistance which does not depend on V_G and can persist even in the absence of the Schottky barrier. This might explain the reduced conductance of CNT using Au contact of around one-third of the conductance quanta.⁹

Figures 2(c)–2(f) show the SBH and tunneling barrier height versus interfacial distance for Pd and Pt. One common feature for these two metals is their negative tunneling barriers around equilibrium distance. So, it is of less concern and the SBH alone determines the contact performance. Pt has a larger work function and less effective bonding so that Fermi level for Pt might be expected to be pinned at a position lower than Pd. However, this is not the case. The dipole moment at the interface depends on the metal species and the detailed atomic geometry, but not directly related to the bonding strength. Detailed charge transfer analysis shows that even though Pd/CNT has stronger bonding, it has a weaker dipole. Charge build-up in the bonding region that comes from the Pd side actually counteracts part of the dipole moment and pushes down the metal levels. Figure 3 shows the charge difference plot along a particular cross section for Pd(111)/CNT and Pt(111)/CNT, respectively. As can be seen from the graph, even though there is less charge build up between Pt and CNT (indicated by less dense mesh in the charge build up region), it is more effective in dipole formation, which brings up the levels on the metal side and pins the Fermi level deeper into the gap. Pd(100)/CNT has the smallest dipole moment and Fermi level is correspondingly pinned nearer to the valence band edge. This leads to its lowest SBH in our study ~ 0.15 eV. This is consistent with experiment that Pd is a preferable metal for making ohmic contact.^{5,6} The finite SB between metal and CNT is due to a small size of the nanotube used in the simulation.

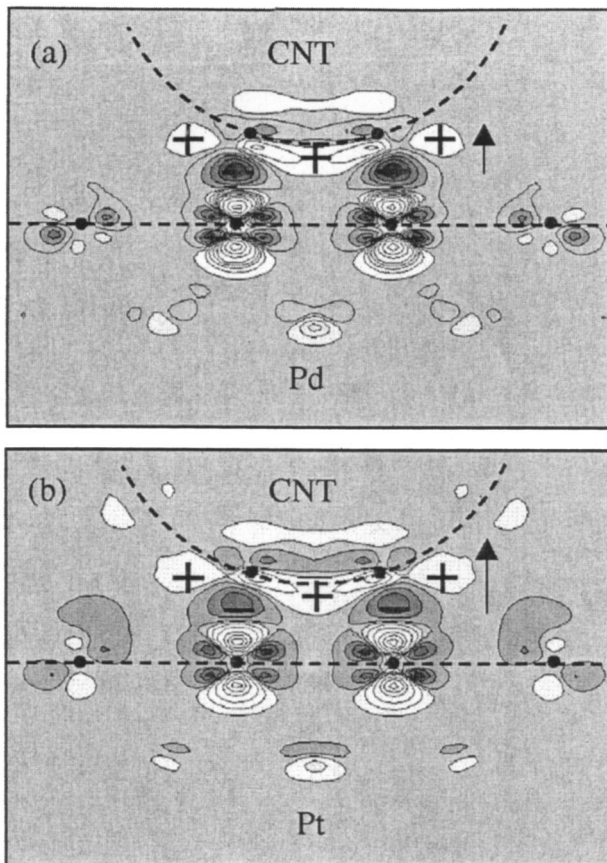


FIG. 3. Charge difference plot along a particular cross section showing charge accumulated (black) and charge depleted (white) region for (a) Pd(111)/CNT, (b) Pt(111)/CNT at their corresponding equilibrium distance. Arrows indicate direction and magnitude of the dipole moment.

There is experimental evidence that Pd makes good ohmic contact to larger diameter nanotubes ($d > 2$ nm) while Schottky persists for smaller diameter nanotubes.¹⁹

We also studied the effect of other degrees of freedom on SBH. They turn out not to influence SBH as much as the interfacial distance and surface orientation. For Pd(111)/CNT contact at equilibrium distance of 2.1 Å, rotation of the CNT changes the SB by less than 0.015 eV. The atomic relaxation at the interface changes the SB by 0.006 eV. Translation along the CNT axis changes the SB by less than 0.02 eV. Also, energy barriers associated with changing these degrees of freedom make these processes energetically unfavorable and further suppress such deviation. So the presence of other degrees of freedom only gives a minor correction to the calculated SBH and will not change our picture of the SBH dependence described above.

In summary, we have studied the SBH at the metal/CNT contact as a function of atomic geometry. It must be emphasized that due to the smallness of the metal/CNT junction, the detailed atomic geometry at the interface may influence the SBH to a considerable degree. Two most important factors are (1) surface orientation. This affects the reactivity of the surface and changes the equilibrium interfacial distance as in the Au case; (2) metal species. This dictates the charge transfer pattern as in the case of Pd and Pt. Both of these two factors are crucial to Schottky barrier height. We suggest that even though MIGS¹⁰ has achieved considerable success in studying bulk metal/semiconductor interface, effects like the detailed atomic geometries should be incorporated to fully understand the electronic structures at the extremely small metal/CNT junction. Our simulation results give insight into the large conductance variation in Au/CNT contact and low SB at the Pd/CNT contact. The capability to model the SBH on the atomic scale opens up new ways that enable us to design better contacts.

ACKNOWLEDGMENTS

This work is supported by NSF grant on Network for Computational Nanotechnology. The authors thank Ali Javey and Hongjie Dai for sharing experimental details and helpful discussions.

*Email address: kjcho@stanford.edu

¹A. Javey, H. Kim, M. Brink, Q. Wang, A. Ural, J. Guo, P. McIntyre, P. McEuen, M. Lundstrom, and H. Dai, *Nat. Mater.* **1**, 241 (2002).
²S. Heinze, J. Tersoff, R. Martel, V. Derycke, J. Appenzeller, and P. Avouris, *Phys. Rev. Lett.* **89**, 106801 (2002).
³S. Heinze, M. Radosavljevic, J. Tersoff, and P. Avouris, *Phys. Rev. B* **68**, 235418 (2003).
⁴J. Guo, S. Datta, and M. Lundstrom, *IEEE Trans. Electron Devices* **51**, 172 (2004).
⁵A. Javey, J. Guo, Q. Wang, M. Lundstrom, and H. Dai, *Nature (London)* **424**, 654 (2003).
⁶D. Mann, A. Javey, J. Kong, Q. Wang, and H. Dai, *Nano Lett.* **3**, 1542 (2003).
⁷V. Derycke, R. Martel, J. Appenzeller, and P. Avouris, *Appl. Phys. Lett.* **80**, 2773 (2002).
⁸A. Bachtold, M. Henny, C. Tarrier, C. Strunk, C. Schonenberger, J. Salvetat, J. Bonard, and L. Forro, *Appl. Phys. Lett.* **73**, 274 (1998).

⁹Y. Yaish, J. Park, S. Rosenblatt, V. Sazonova, M. Brink, and P. McEuen, *Phys. Rev. Lett.* **92**, 046401 (2004).
¹⁰J. Tersoff, *Phys. Rev. B* **32**, 6968 (1985).
¹¹M.C. Payne, M.P. Teter, D.C. Allan, T.A. Arias, and J.D. Joannopoulos, *Rev. Mod. Phys.* **64**, 1045 (1992).
¹²V.G. Zavodinsky and I.A. Kuyanov, *J. Appl. Phys.* **81**, 2715 (1997).
¹³R.G. Dandrea and C.B. Duke, *J. Vac. Sci. Technol. A* **11**, 848 (1993).
¹⁴J. Appenzeller, J. Knoch, R. Martel, V. Derycke, S. Wind, and P. Avouris, *IEEE Trans. Nanotechnol.* **1**, 184 (2002).
¹⁵J.J. Palacios, A.J. Perez-Jimenez, E. Louis, E. San Fabian, and J.A. Verges, *Phys. Rev. Lett.* **90**, 106801 (2003).
¹⁶F. Leonard and J. Tersoff, *Phys. Rev. Lett.* **84**, 4693 (2000).
¹⁷S. Peng and K.J. Cho, *MRS Symp. Proc.* **675**, W4.8 (2001).
¹⁸Y. Zhang and H. Dai, *Appl. Phys. Lett.* **77**, 3015 (2000).
¹⁹A. Javey, Q. Wang, W. Kim, and H. Dai, *IEDM Technical Digest* 741 (2003).